Spectroscopic Studies of the Intermediates in the Conversion of 1,4,11,12-Tetrahydro-9,10-anthraquinone to 9,10-Anthraquinone by Reaction with Oxygen under Basic Conditions

Saba M. Mattar,* Abdul H. Emwas, and Larry A. Calhoun

Chemistry Department, University of New Brunswick, Fredericton, New Brunswick, Canada E3B6E2

Received: April 8, 2004; In Final Form: August 26, 2004

The intermediates of the 1,4,11,12-tetrahydro-9,10-anthraquinone (THAQ) to 9,10-anthraquinone (AQ) reaction are studied by various spectroscopic and computational methods. X-ray diffraction, two-dimensional nuclear magnetic resonance (NMR) spectroscopy, and geometry optimization calculations, by the UB1LYP hybrid density functional technique, show that THAQ initially exists in the keto form (*cis*THAQK). Addition of very small amounts of NaOH to *cis*THAQK in solution catalytically converts it into the corresponding enol form (THAQE). The THAQE is then oxidized, by dissolved O_2 in solution, to give the novel 1,4-dihydro-9,10-anthraquinone (DHAQ) which is isolated, and its single-crystal structure is characterized by X-ray spectroscopy. If NaOH is added to THAQE, the 1,4-dihydro-9,10-anthrasemiquinone (DHASQ) radical anion is produced. It is detected by electron paramagnetic resonance (EPR) spectroscopy, and its experimental nuclear hyperfine coupling constants are correlated with those computed by the UB1LYP method. Consequently, the production of DHASQ radical anions, upon addition of NaOH, follows the stepwise reaction *cis*THAQK $\rightleftarrows$ THAQE $\rightleftarrows$ DHASQ. The treatment of DHAQ with NaOH in methanol also generates the DHASQ radical proving that DHAQ is a precursor to DHASQ. It is thus shown that the DHASQ radical anion can be generated either by oxidation of the THAQE or the single electron reduction of the DHAQ. When the DHASQ radical anion is exposed to small amounts of O_2, it is converted into the corresponding 9,10-anthrasemiquinone (ASQ). Further O_2 oxidizes this radical anion to AQ. This proves that DHASQ must first form the ASQ intermediate before being converted to AQ. These results reveal that the THAQ−soda pulping process, in the presence of atmospheric O_2, first produces AQ. From then onward it is the same as the popular AQ−soda pulping process used in the paper manufacturing industry.

1. Introduction

As an extension of our study of naturally occurring *para*-quinones, we have also been investigating even larger ones, such as 9,10-anthraquinone (AQ), 10,10′-bianthronylidene, and 1,4,-11,12-tetrahydro-9,10-anthraquinone (THAQ).[1−4] In addition to undergoing redox reactions of commercial interest, these larger quinones also experience important structural and conformational changes during their reduction to the corresponding radical anions.[2,3]

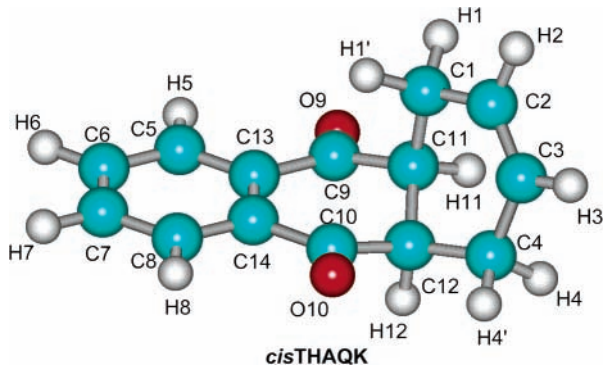

***cis*THAQK**

AQ has been used as a catalytic accelerator in alkaline wood pulping.[5−7] In an effort to understand the catalytic role of AQ in this process, various mechanisms have been proposed. In one mechanism, an adduct formed between the lignin quinone-methide and AQ was believed to be a key intermediate.[8] A second mechanism suggested the involvement of the 9,10-anthrasemiquinone (ASQ) radical anion as an intermediate catalyst.[1,9−11] This assumption was based on the fact that the ASQ was found to be stable in aqueous alkaline media up to 130 °C and could be generated by wood and cellulose in alkaline and Kraft pulping.[1,9,10] Alkaline-AQ pulping is still used in the delignification of wood worldwide. However, the exact catalytic mechanism of AQ is still an open question, and research into this important commercial process is ongoing.[12]

THAQ is prepared by the [4 + 2] cycloaddition of 1,4-naphthaquinone with butadiene in nonpolar solvents and is a precursor in the synthesis of AQ. The AQ is then prepared from THAQ by oxidation.[13] It is therefore reasonable to attempt to use THAQ, in the presence of atmospheric oxygen, as an additive in the alkaline pulping of wood instead of AQ. The yields of this process were found to be very similar to that of alkaline-AQ pulping.[14−15]

The conversion of THAQ to AQ is a complex reaction in which four hydrogen atoms are lost and the THAQ is oxidized. Logically, this is a multistep process that must involve more than one reaction intermediate. We have previously used electron paramagnetic resonance (EPR) spectroscopy to identify the 1,4-dihydro-9,10-anthrasemiquinone **(**DHASQ**)** radical intermediate in this oxidation process.[4] The DHASQ was characterized by

* To whom correspondence should be addressed. E-mail: mattar@unb.ca.

10.1021/jp040280v CCC: $27.50 © 2004 American Chemical Society
Published on Web 12/08/2004

simulating its EPR spectrum and correlating its isotropic proton hyperfine tensor components, $a^{iso}(^1H)$, with those calculated using the UB1LYP hybrid density functional method.

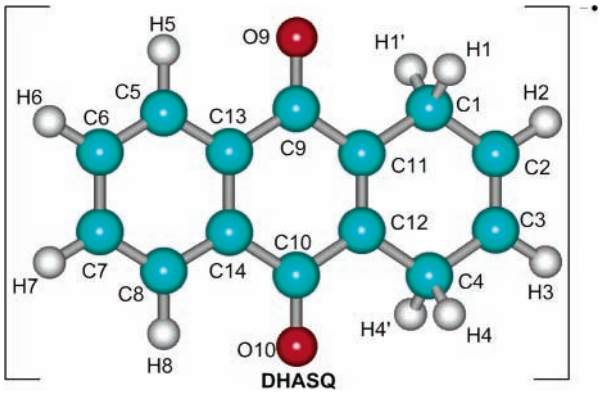

Significant to the oxidation reaction mechanism is whether the THAQ molecule is initially in the *cis*-keto (*cis*THAQK), *trans*-keto (*trans*THAQK), or *trans*-enol (THAQE) form. It is not known which of these forms is prevalent in the solid state or in various solvents.

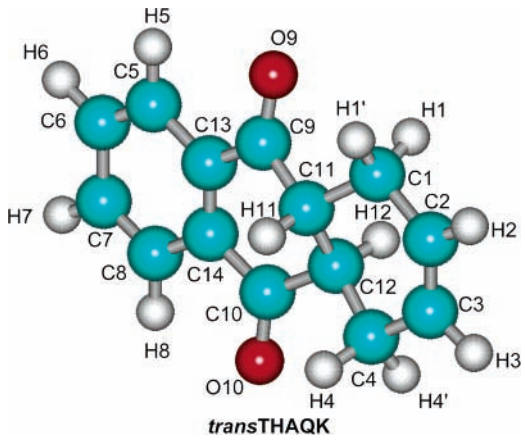

Furthermore, at ambient temperatures, it was not known beforehand whether the *cis*THAQK, *trans*THAQK, and THAQE tautomerization is rapid or slow. The electron affinities and ionization energies are expected to be different for each molecule. Consequently, their oxidation and reduction reactions are also expected to differ.

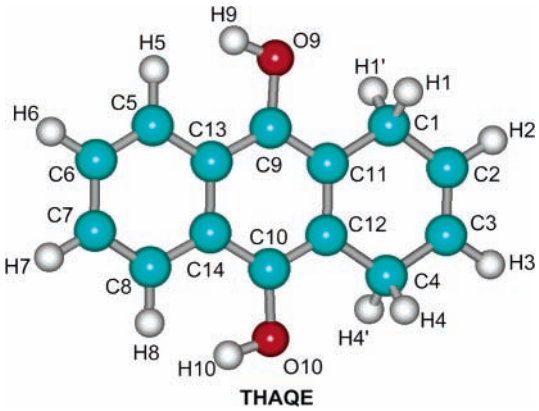

In going from *cis*THAQK or *trans*THAQK to THAQE, a rehybridization of the C11 and C12 atoms from sp^3 to sp^2 must occur. This may not be a simple process for a three-fused-ring molecule. For these reasons, we have opted to further study the

$$\text{THAQK} \rightleftarrows \text{THAQE} \rightarrow \text{AQ}$$

system and attempt to characterize the structure of all of its intermediates.

In section 2, the experimental details and computational techniques are described. This is followed, in subsection 3a, by the comparison of the *cis*THAQK X-ray and computed structures. The conversion of *cis*THAQK to THAQE and the assignment of their liquid-phase structures by 1-D and 2-D NMR is then discussed in subsections 3b and 3c. In subsection 3d, the DHASQ radical anion is then generated from both the THAQE and DHAQ intermediates. The DHASQ EPR spectra are simulated, and the average hyperfine and **g** tensor components are compared with those computed by the UB1LYP hybrid density functional method. The effects of the solvent on the EPR spectra are also presented. Finally, in subsection 3e the proposed reaction mechanism of the oxidation of *cis*THAQK to AQ including its three intermediates is described. Section 4 summarizes the findings and conclusions of the whole study.

2. Experimental Details

The NMR spectra were recorded on a UNITY 400 MHz Varian spectrometer, equipped with a 5 mm inverse detection probe. Data acquisition and manipulation were carried out by means of the Varian VNMR version 4.3A software running on a SUN model IPX work station. For all two-dimensional (2-D) experiments, the spectra were recorded at 25 °C, while for the one-dimensional (1-D) experiments the temperature was varied from −70 to 50 °C. Typically, the 1-D ^1H spectra had a spectral width of 5599.9 Hz, and the number of data points acquired was 41,856. The corresponding ^{13}C spectra consisted of 59 968 data points, and the spectral width was 25 000.0 Hz.

The proton-detected 2-D $^1H-^{13}C$ heteronuclear multiple-quantum coherence (HMQC) spectra were recorded at 25 °C. The ^1H spectral width was 3370.1 Hz. The number of data points was 1984 and zero filled to 4096. The ^{13}C spectral width was 1373.1 Hz. To perform the 2-D Fourier transform, the increments were zero-filled to 1024 points. Sixteen transients were acquired per increment. The polarization transfer delay was optimal for $^1J_{CH} = 140$ Hz. The relaxation delay time was 2.0 s. A standard WALTZ-16 sequence was employed for ^{13}C decoupling.[16] A similar setup was used for the long-range proton-detected heteronuclear-multiple-bond-correlation (HMBC) experiments, except no ^{13}C decoupling was used and the polarization transfer delay was optimal for $^nJ_{CH} = 8$ Hz ($n = 2,3$).

To investigate the keto−enol tautomerism, 0.0213 g of *cis*THAQK was dissolved in 700 μL of the appropriate solvent. This was followed by adding 4 μL of 0.1 M NaOH, in D_2O, and the NMR spectra were recorded.

Low resolution mass spectra were generated with a Kratos MS 50TC mass spectrometer. The samples were directly injected into the system and the chamber heated from 30 to 220 °C at a rate of 20 °C/min. Sample ionization was carried out via electron impact at an energy of 71.6 eV. The operating base pressure was 2.0×10^{-7} atm.

The EPR spectra of the radical intermediates were recorded on a Varian E104 and a Varian E9 spectrometer described previously.[17−21] The microwave power incident on the sample was 1.0 mW, and the magnetic field was modulated at 100 kHz. The modulation amplitude was always less than one tenth of the peak-to peak line widths. A Bell 640 Gaussmeter was used

to calibrate the magnetic field while the microwave frequency was measured by an EIP 371 microwave frequency counter. The spectra were scanned and recorded by means of a computer equipped with a National Instruments AT-MIO-16E-10 data acquisition board and a PHAROS Technologies software program.[18] The spectra were then simulated by a shareware version of the Bruker SIMFONIA-WINEPR software package.

The quinones were dissolved in the appropriate solvent to form approximately 1.0 mM solutions in 25 mL. After purging the solutions with N_2 for 15 minutes, the radicals were then generated by adding 50 μL of 0.5 M NaOH in the absence of air. The solutions were kept under oxygen-free nitrogen and were then transferred into the rectangular TE_{102} EPR cavity via a Teflon tube passing through its center. Successive samples were flushed and new ones introduced into the cavity without exposing the parent solutions to any O_2 by controlling the N_2 pressure. The resulting radicals under these experimental conditions were found to be stable for at least 10 days.

*cis*THAQK was purchased from Aldrich and recrystalized three times from hot 95% ethanol. The final crystals were grown from anhydrous methanol. The DHAQ was synthesized by adding a small amount of NaOH base, in the molar ratio of 1:350, to 21.3 mg of *cis*THAQK dissolved in 1 mL of deuterated methanol. The resulting solution was left to stand for three weeks until well formed reddish-orange crystals of DHAQ settled out. The crystal structure data for *cis*THAQK and DHAQ were recorded with a Bruker AXS P4/SMART 1000 and a Rigaku AFC5R diffractometer, respectively.

The computation of the optimal geometries was carried out using the GAUSSIAN 98W suite of programs.[22] The unrestricted hybrid density functional (UB1LYP) of Adamo and Barone[23,24] was used to determine both the optimal geometries and the total nuclear hyperfine tensors. It consists of the Lee−Yang−Parr correlation functional in conjunction with Hartree−Fock−Becke hybrid exchange functional. The optimizations were carried out with the 6-31G(d) basis set and were terminated when the sum of the energy gradients was less than 0.0005 kcal C^{-1} mol^{-1}.

Although very good geometries may be obtained using the smaller 6-31G(d) basis sets, we have opted for Barone's larger basis sets when calculating the hyperfine tensors.[25] These basis sets are optimized for accurate hyperfine tensor computations of the H, C, and O centers. The UB1LYP results surpass in quality the more expensive ab initio methods at the unrestricted Hartree−Fock (UHF) level.[4,23,24,26−28]

To include the effects of the methanol and DMSO solvents on the computed hyperfine and **g** tensors, the UAHF-PCM method was used.[28,29]

3. Results and Discussion

3a. Comparison of the THAQK Single Crystal and Computed Structures. The single crystal structure of THAQ, obtained by X-ray diffraction after recrystallization from methanol, indicates that it exists in the bent and twisted *cis*THAQK form. This is consistent with its preparation by the [4 + 2] cycloaddition of butadiene to naphthaquinone. The single crystal structure, refinement parameters, bond lengths, angles, atomic coordinates, and their equivalent isotropic displacement parameters are listed in detail elsewhere.[30]

The atom numbering and structure of the molecule is shown in Figure 1. The C═C bond distance between C2 and C3 is 1.318(2) Å which is in agreement with similar ethylenic double bonds.[31] The average of the C1−C11 and C4−C12 bond lengths is 1.526 Å. It also agrees with the normal values of similar bonds of sp^3 hybridized carbon atoms[32] and is quite a bit longer than

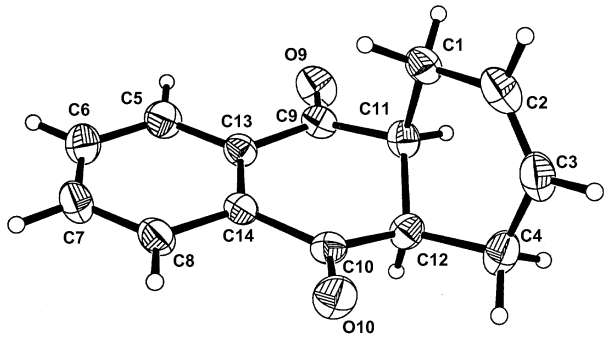

Figure 1. Structure and atom numbering of 1,4,11,12-tetrahydro-9,-10-anthraquinone (*cis*THAQK).

those within the C5, C6, C7, C8, C14, C13 arene ring. In addition, due to the sp^3 hybridization of the C11and C12 atoms, their bond distance is 1.5335(16) Å and characteristic of a typical single carbon−carbon bond. The distances between the sp^2 and sp^3 carbons are 1.4952(17) Å for C1−C2 and 1.4830(2) Å for C3−C4.

The C5, C6, C7, C8, C14, C13 arene ring is planar and is not affected by the bent and twisted conformation of the C1, C2, C3, C4, C12, C11 ring. As a result of the bent conformation of the latter ring, the angles around the sp^2 alkene carbons, C2 and C3, are larger than 120°. For example, the C1−C2−C3 angle is 124.12(12)°, and the C2−C3−C4 angle is 123.83(12)°.

The UB1LYP HDF geometry optimization of THAQ, starting with H11 and H12 on the same side of the molecule, also predicts *cis*THAQK as the most stable form. The computed and experimental bond lengths and angles show that both are in very good agreement and have the same conformation. The maximum of the difference between the computed and experimental bond lengths is less than 0.025 Å; for bond angles it is less than 1.0°. Consequently, the UB1LYP/6-31G(d) method reproduces the experimental geometry quite well.

The conversion from *cis*THAQK, where both H11 and H12 are on the same side (face) of the molecule, to *trans*THAQK, where they are on the opposite sides, is impossible without going through the THAQE intermediate or explicitly breaking bonds. The formation of *cis*THAQK pure single crystals from neutral solutions, as evidenced by X-ray diffraction, is a strong indication the keto−enol tautomerism

$$\textit{cis}\text{THAQK} \rightleftarrows \text{THAQE} \rightleftarrows \textit{trans}\text{THAQK}$$

does not readily occur. Since the single crystal structure may only represent one of a number of tautomeric species in solution, NMR spectroscopy is used to determine if THAQ in various solvents, in addition to the recrystallization solvent (95% ethanol), also exists as *cis*THAQK and if it tautomerizes to THAQE in the range −50 to 70 °C.

3b. Assignment of the ^{1}H and ^{13}C NMR Spectra of THAQ. To the best of our knowledge, the ^{1}H and ^{13}C NMR spectra for both *cis*THAQK and THAQE have not been reported. Thus, it is important to first assign their individual spectra before studying their tautomerization.

All ^{1}H NMR spectra of *cis*THAQK in various solvents, between −50 and 70 °C, consist of 6 different peaks as listed in Table 1. Integration of each of these peaks shows that they are due to the same number of protons. This is not consistent with the suggested *cis*THAQK structure or that determined by X-ray crystallography and predicted by the UB1LYP computations. In addition, THAQE is expected to give only five distinct peaks and is therefore ruled out as a possible structure. The only remaining possibility is that in the liquid state the

TABLE 1: ^{1}H and ^{13}C Chemical Shifts[a] of THAQK in Various Solvents at 298 K

equivalent atoms	acetone	chloroform	DMSO	methanol
		^{1}H Chemical Shifts		
H1, H4	2.47	2.55	2.45	2.32
H1′, H4′	2.23	2.26	2.22	2.15
H2, H3	5.70	5.75	5.70	5.66
H5, H8	8.00	8.06	8.01	7.94
H6, H7	7.85	7.76	7.80	7.85
H11, H12	3.49	3.42	3.44	3.49
		^{13}C Chemical Shifts		
C1, C4	24.08	24.47	24.37	23.96
C11, C12	46.16	46.58	46.07	46.29
C2, C3	124.61	124.59	125.11	124.27
C5, C8	126.40	126.88	126.79	126.26
C13, C14	134.09	134.02	134.03	133.97
C6, C7	134.22	134.28	135.05	134.12
C9, C10	197.20	198.08	198.20	198.10

[a] Chemical shift in parts per million (ppm).

SCHEME 1: Rapid Averaging of *cis*THAQK in Solution

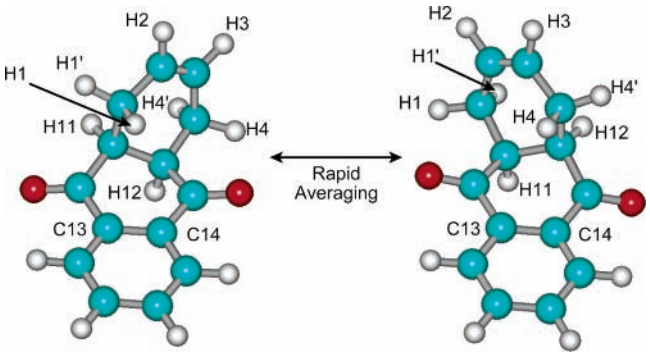

*cis*THAQK fluctuates between two bent conformations to give the average structure shown in Scheme 1. This renders the (H1, H4), (H1′, H4′), (H2, H3), (H5, H8), (H6, H7), and (H11, H12) as six distinct equivalent pairs.

The ^{1}H and ^{13}C NMR spectra of THAQK were interpreted using standard 2D methodology (Table 1). The (H2, H3) and (H11, H12) pairs of resonances were unequivocally assigned by inspection. The observation of a correlation in the HMBC spectrum between the ^{1}H resonance at 8.00 ppm with the carbonyl carbon signal at 197.2 ppm identifies this resonance as due to the (H5, H8) protons. Consequently, the resonance at 7.85 ppm results from the (H6, H7) pair. A nuclear Overhauser effect (NOE) experiment is used to assign the peaks at 2.26 and 2.25 ppm belonging to the aliphatic (H1, H4) and (H1′, H4′) pairs of resonances. When the (H11, H12) signals occurring at 3.49 ppm are saturated, the maximum enhancement is observed for the lines around 2.45 ppm. This indicates that they are due to the closest nuclei and should be assigned to H1 and H4. Consequently, the remaining 2.23 ppm peak must be due to (H1′, H4′) resonances.

The assignment of most of the ^{13}C spectrum followed from the HMQC spectrum, shown in Figure 2, in a straightforward manner. The ^{13}C chemical shift of the remaining quaternary carbons (C13, C14) is extremely close to that of the (C6, C7) pair. It was assigned to the resonance at 134.09 ppm on the basis of the intensity of the signal relative to the protonated carbons and the absence of a correlation involving this chemical shift in the HMQC spectrum.

Since all the NMR spectra in the temperature range −50 to 70 °C have the same number of peaks and are due to *cis*THAQK, then it is safe to assume that the

$$\textit{cis}\text{THAQK} \rightleftarrows \text{THAQE} \rightleftarrows \textit{trans}\text{THAQK}$$

keto−enol tautomerization does not easily occur under these neutral conditions and temperatures.

3c. Conversion of cisTHAQK to THAQE. From our earlier work, it was found that the addition of NaOH to a solution of **THAQ**, in the ratio of 1:1, resulted in the rapid formation of the **DHASQ** radical anion.[4] In an attempt to slow this complex reaction, the ratio of NaOH/THAQ was reduced by 2 orders of magnitude. The proton spectrum, in Figure 3a, is obtained by adding 1 equiv of NaOH/D_2O solution to 350 equiv of **THAQK** in methanol-d_4. Initially, the six familiar **THAQK** peaks plus a new HOD line at approximately 4.9 ppm, arising from the exchange between NaOH and D_2O, are apparent. In addition, there is no evidence of any paramagnetic species in solution.

As the spectra were monitored as a function of time, four new lines appeared at 3.50, 5.97, 7.35, and 8.12 ppm as shown in Figure 3b−d. The intensities of the new lines slowly increased while the those of the original six decreased. Figure 3d indicates that after 4320 min all the original THAQK peaks have

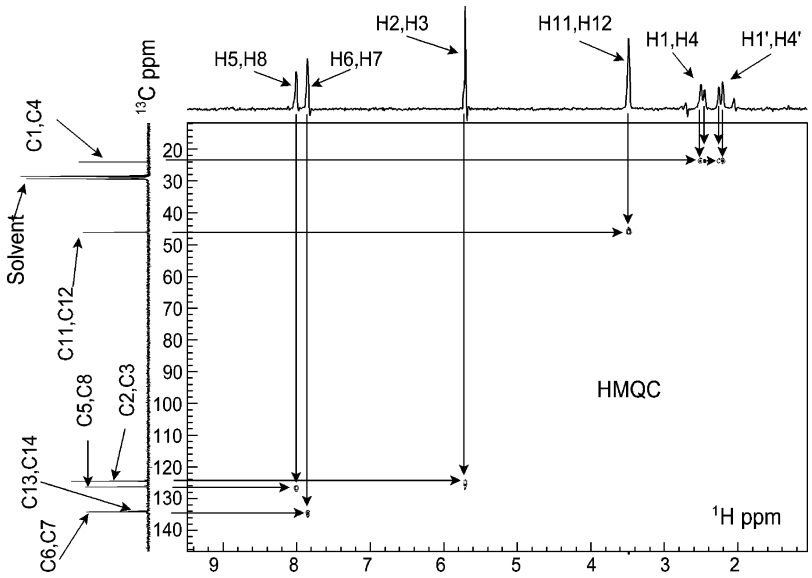

Figure 2. ^{1}H, ^{13}C, and ^{1}H−^{13}C HMQC NMR spectrum of *cis*THAQK in acetone-d_6.

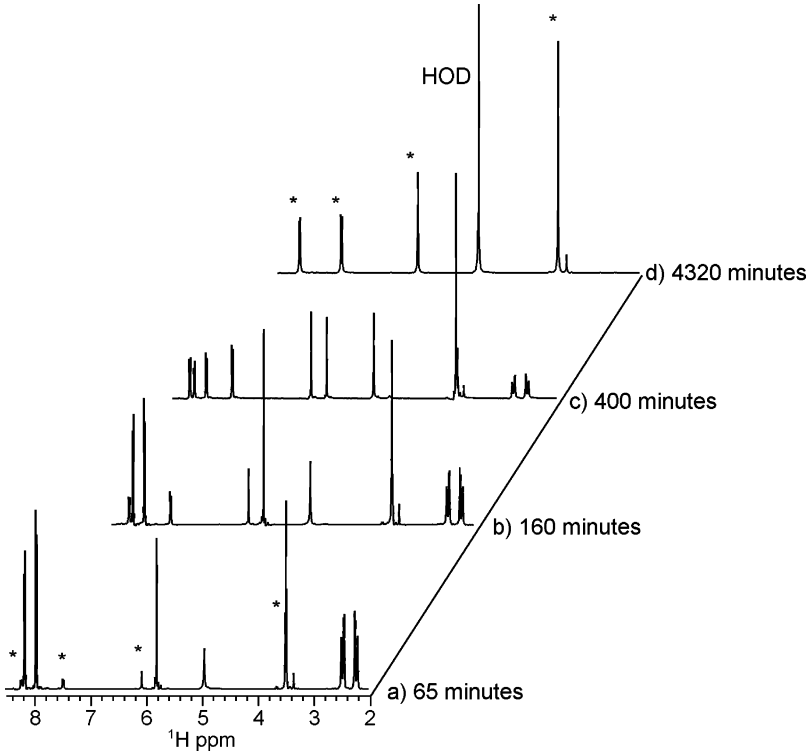

Figure 3. The 400 MHz ^{1}H NMR spectra showing the conversion of *cis*THAQK to THAQE as a function of time. THAQE lines are indicated by an asterisk.

TABLE 2: ^{1}H and ^{13}C Chemical Shifts[a] of THAQE in Methanol at 298 K

H1,H4	H2,H3	H5,H8	H6,H7	H9,H10
3.50	5.97	8.12	7.35	8.40[b]

C1,C4	C2,C3	C5,C8	C6,C7	C9,C10	C11,C12	C13,C14
24.20	123.31	121.02	123.68	142.02	117.51	124.68

[a] Chemical shift in parts per million (ppm). [b] Determined from the NMR spectrum in DMSO.

disappeared and only four new peaks are apparent. Integration of the areas under the spectral lines showed that the number of protons of the 3.50 peak were double each of the other three. The NMR spectra also indicate that *cis*THAQK was converted to a single new product and no intermediate species were apparent.

Assuming that the resulting molecule is THAQE, then five proton peaks instead of four are expected. However, the OH moiety of the THAQE undergoes fast exchange with the labile OD group of the CD_3OD solvent and causes its corresponding peak to disappear. To verify this, the experiment was repeated in DMSO-d_6, where the deuterium exchange is not as fast. Indeed, in this case the resulting ^{1}H NMR spectra displayed an OH proton peak around 8.4 ppm.

The ^{1}H and ^{13}C spectra of THAQE were assigned in a manner similar to that used for the THAQK. The chemical shifts are listed in Table 2. The entire ^{1}H spectrum was assigned by inspection. The protonated carbon atoms were clearly identified from the HMQC spectrum. The chemical shifts of the quaternary carbons (C9, C10), (C11, C12), and (C13, C14) were found to be 142.02, 117.51, and 124.68 ppm, respectively. They are based on the HMBC ^{1}H/^{13}C correlations occurring between the (8.12/142.02), (5.97/117.51), and (7.35/124.68) ppm peaks.

It is important to note that a very small amount ($^1/_{350}$ equiv) of NaOH was required to convert the *cis*THAQK to THAQE. This indicates that the hydroxyl ion acts as a catalyst. A plausible mechanism for the enolization process (in water) is given in Scheme 2. The absence of any intermediates suggests that once one CO group has been converted to C−O−H then the conversion of the second CO group to a hydroxyl is expected to be much faster than the first.

A similar reasoning also holds when the solvent is methanol.

3d. Electron Paramagnetic Resonance of the DHASQ Radical Anion. The addition of a small amount of NaOH to THAQK using methanol-d_4 as a solvent enabled us to gradually convert the parent THAQK to THAQE. However, if the ratio of NaOH/THAQK is increased to 1:4, the THAQK NMR spectrum disappears due to the formation of a paramagnetic free radical species in solution.

To shed more light on this radical, the reaction was repeated in DMSO, and the EPR spectra of the products were recorded. The resulting spectrum was found to be identical to that recorded previously by Mattar and Stephens.[4] This indicates that the THAQK molecule first converts into THAQE and in the presence of more OH^- subsequently forms the DHASQ radical anion. This last step is still a complex one which involves the loss of two protons and an oxidation. Therefore, it is quite probable that an additional reactive intermediate is involved.

There are two possible routes by which the THAQE molecule is converted into the DHASQ radical anion. The first entails the conversion of THAQE to the corresponding DHAQ molecule in the presence of O_2. This is then followed by a single electron reduction to the DHASQ radical. In the second mechanism, THAQE is first converted to the DHAQ dianion which is oxidized back to the DHASQ anion. This is depicted in Scheme 3.

The second route requires 2 equiv of OH^- to form the DHAQ dianion, making the first mechanism the most probable one. In order to prove that the first mechanism is operational, it is crucial to isolate the DHAQ intermediate and then reduce it with OH^- to the corresponding DHASQ radical. In addition, Scheme 3

SCHEME 2: Enolization of THAQK by OH− in an Aqueous Medium

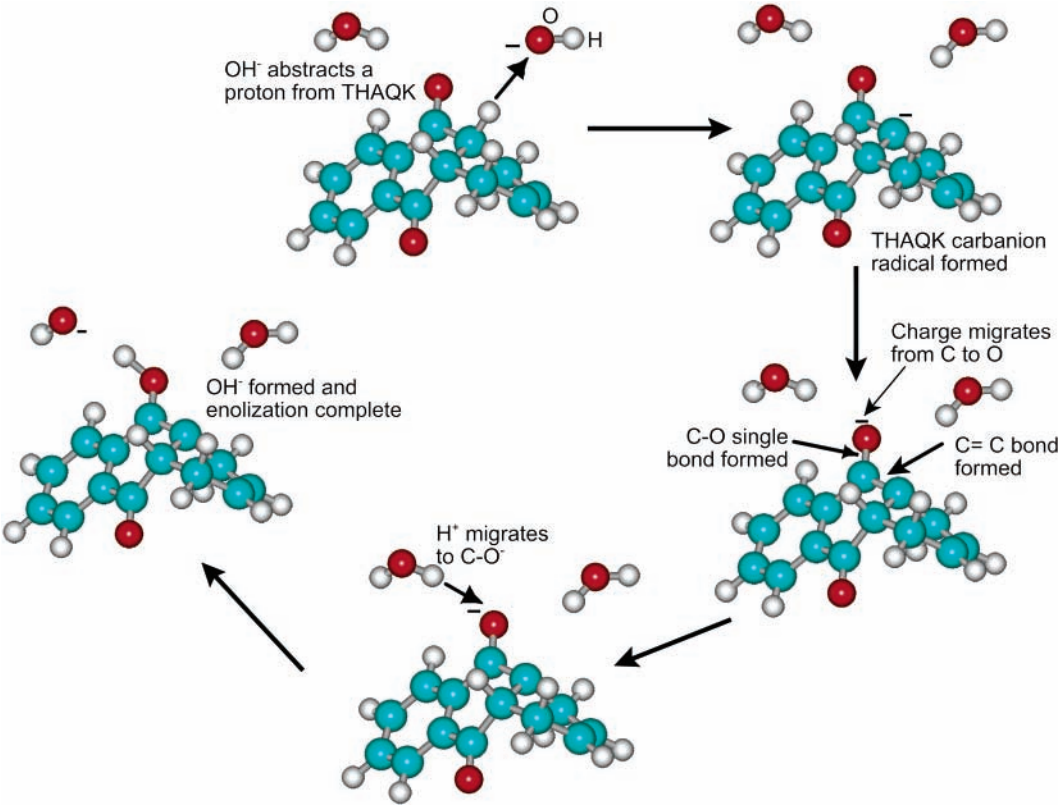

SCHEME 3: Conversion of THAQE to the DHASQ Radical Anion.

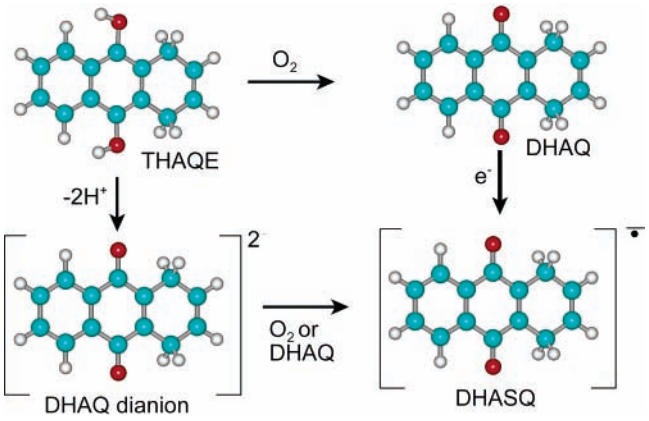

does not exclude the possibility of the

$$\mathrm{DHAQ} + \mathrm{DHAQ}^{2-} \rightarrow 2\mathrm{DHAQ}^{\bullet -}$$

comproportionation reaction.

DHAQ was prepared by dissolving THAQK in methanol-d_4 and adding NaOH in the molar ratio 350:1, respectively. This small amount of base converted the original THAQK to THAQE. The solution was left to stand for three weeks until well formed orange crystals settled out and their structure was determined by X-ray crystallography. It revealed that they are indeed DHAQ crystals, and crystallize in the orthorhombic space group. Their unit cell parameters were found to be $a = 16.354(3)$ Å, $b = 12.612(2)$ Å, and $c = 4.914(3)$ Å. An ORTEP diagram of the crystal structure is given in Figure 4. Its refinement parameters, bond lengths bond angles, atomic coordinates, and their equivalent isotropic displacement parameters are given in ref 30.

The crystal structure shows that in going from THAQK to DHAQ the molecule still maintains its keto structure because its C9, O9 and C9′, O9′ distances are 1.222(4) Å and are typical of CO double bonds. They are also in agreement with previously published values on similar compounds.[33] The aromatic ring angles are similar to those of THAQK and range from 119.3-(4) to 120.0(4) Å. They are also in good agreement with those of analogous structures determined by Phillips and Trotter.[31] Because the C1−C11 bond in THAQK is converted from an sp^3-sp^3 type to an sp^3-sp^2 in DHAQ, its bond distance decreases from 1.5299(1) to 1.478(6) Å. The sp^3-sp^2 C1−C11 and C1−C2 bond lengths are 1.478(4) and 1.447(5) Å, respectively. They are longer than the corresponding sp^2-sp^2 C2−C3 bond length of 1.324(9) Å.

The isolation of the DHAQ in pure form, as single crystals, enables us to verify if it can be converted into the corresponding DHASQ radical anion via a single electron reduction. When

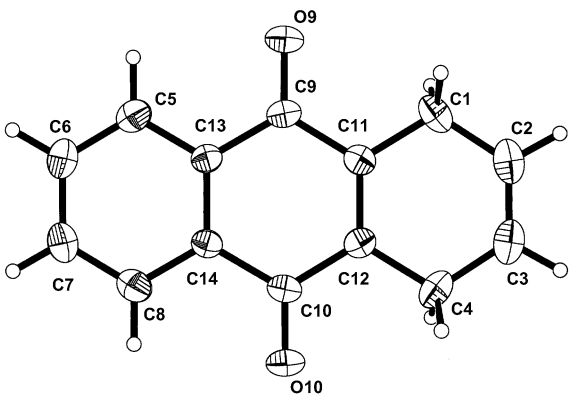

Figure 4. ORTEP diagram of the DHAQ structure and numbering of its unique atoms.

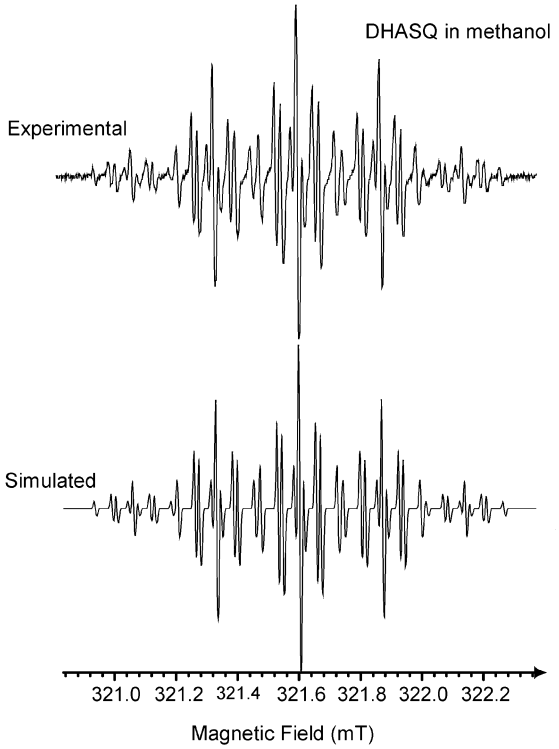

Figure 5. Experimental and simulated EPR spectra of the DHASQ radical obtained by the addition of 1 equiv of NaOH to DHAQ in oxygen-free methanol.

the pure DHAQ crystals were dissolved in DMSO-d_6, to form a 1.0 mM solution, and 1 equiv of NaOH was added, the resulting EPR spectrum was again identical to that determined previously by Mattar and Stephens.[4] This unequivocally proves the formation of the DHASQ radical anion. Therefore, the first proposed mechanism is certainly possible.

Since the DHAQ was originally produced and isolated starting from THAQK in methanol, it is imperative to further prove that the DHASQ radical may also be generated by starting from DHAQ in methanol. The EPR spectrum obtained by adding 1 equiv of NaOH to a 1.0 mM solution of DHAQ in methanol is shown in Figure 5. The splitting patterns and intensities of this spectrum do not resemble those of the DHASQ radical in DMSO. However, from such an observation alone, it is insufficient to conclude that this radical is not the DHASQ radical anion.

Due to the large number of overlapping lines in a very small region of the EPR spectrum, any slight variation in the ^{1}H hyperfine coupling constant, $a^{iso}(^1H)$, will lead to large changes in their overall intensity patterns. The proper way to determine the nature of this new radical is to simulate its experimental spectrum and compare the resulting $a^{iso}(^1H)$ with those previously simulated by Mattar and Stephens.[4] Table 3 lists the experimental and computed $a^{iso}(^1H)$ of the DHASQ radicals in DMSO and methanol. It reveals that the experimental $a^{iso}(^1H)$, obtained by simulation of the spectra (Figure 5 and Figure 2b of ref 4), are very close in magnitude. The maximum difference of $a^{iso}(^1H)$ between them is only 0.23 G and occurs on the H2 and H3 nuclei. These small differences in the hyperfine coupling constants are attributed to the different solvents.

The tails of an EPR spectrum are usually the regions that are best resolved and suffer minimal resonance overlap. Therefore, although they have low intensities, they are the most appropriate regions to demonstrate the different patterns of DHASQ in

TABLE 3: ^{1}H Hyperfine Coupling Constants[a] for 1,4-Dihydro-9,10-anthrasemiquinone

		methanol		DMSO	
	GP[b]	expt[c,d]	calcd	expt[c,e]	calcd
^{1}H1	2.240	|2.69|	2.343	|2.70|	2.396
^{1}H1′	2.240	|2.69|	2.343	|2.70|	2.396
^{1}H2	-0.027	|0.04|	-0.135	|0.05|	-0.143
^{1}H3	-0.027	|0.04|	-0.135	|0.05|	-0.143
^{1}H4	2.240	|2.69|	2.343	|2.70|	2.396
^{1}H4′	2.240	|2.69|	2.343	|2.70|	2.396
^{1}H5	-0.158	|0.55|	-0.264	|0.32|	-0.191
^{1}H6	-0.937	|0.70|	-0.882	|0.75|	-0.905
^{1}H8	-0.158	|0.55|	-0.264	|0.32|	-0.191
^{1}H7	-0.937	|0.70|	-0.882	|0.75|	-0.905

[a] Values in Gauss: 1.0 G = 10^{-4} Tesla. [b] GP denotes a gas phase computation with no solute−solvent interactions. [c] The signs of the hyperfine coupling constants (HCCs) were not experimentally determined. [d] The DHASQ hyperfine coupling constants were determined from the simulated spectrum in Figure 5. [e] Reference 4.

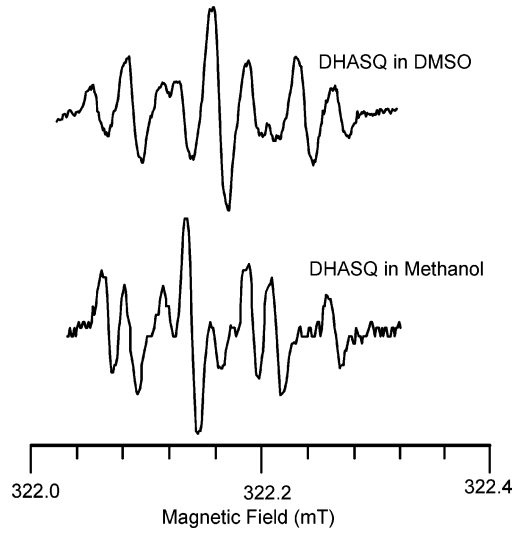

Figure 6. Comparison of the expanded region of the EPR spectrum of DHASQ in DMSO and methanol. Although the differences in the hyperfine coupling constants are minimal, the appearance of the two spectra are quite different.

DMSO and methanol. Figure 6 compares the spectral differences in these two solvents in the high field region between 3220 and 3224 G. Although the differences in the hyperfine coupling constants are very small, the spectra are quite distinct.

The net spin density and $a^{iso}(^1H)$ of the DHASQ radical were previously computed in the gas phase, in the absence of solute−solvent interactions.[4] In this study, we have also included the solvent effects. Table 3 lists the computed $a^{iso}(^1H)$ in the gas phase, methanol, and DMSO. The accuracy of the computed results is very good compared to those of the radical anions of similar quinones, where the uncertainty is usually 2−3 G. In all the computations listed in Table 3, the maximum difference between the calculated and experimental $a^{iso}(^1H)$ is 0.46 G. This occurs for the four equivalent H1, H1′, H4, and H4′ nuclei in the gas phase and the experimental spectrum in DMSO. As the effects of the methanol and DMSO solvents are included in the UB1LYP computations, the agreement between the computed and experimental values gets even better. Although the inspection of Table 3 shows that the relative differences between the experimental and computed values are large, the absolute accuracy is excellent. This is because the differences are less than 0.5 G, while in general the range of possible $a^{iso}(^1H)$ values

SCHEME 4: Intermediates Involved in the Conversion of THAQ to AQ.

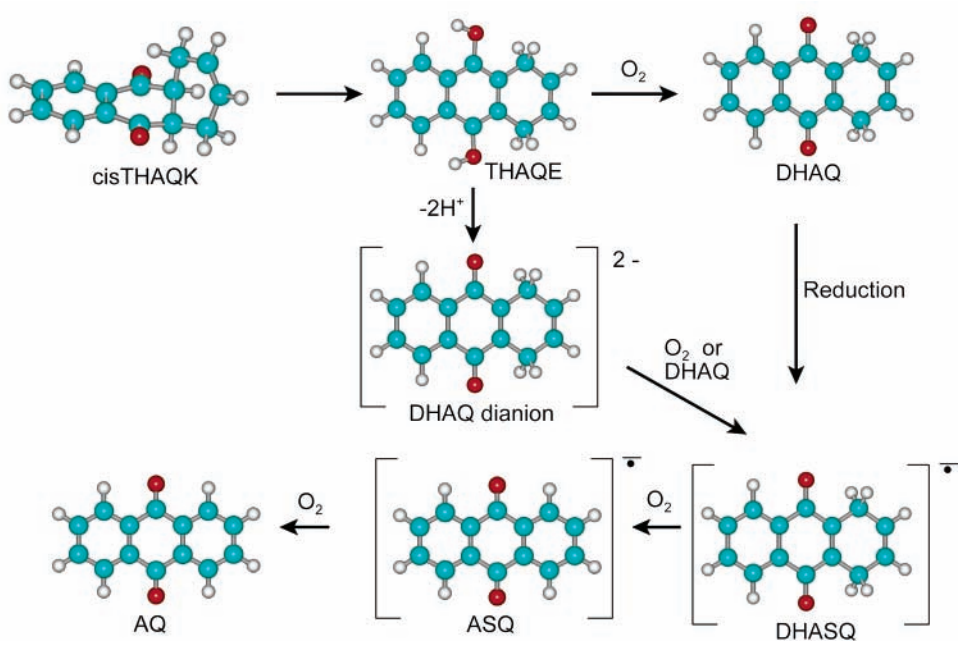

varies from 505.0 G, for a free hydrogen atom, to approximately 42 mG in the case of 2,3,5,6-tetramethoxy-1,4-benzosemiquinone.[18]

One can also safely compare the trends of the experimental and computed $a^{iso}(^1H)$ in different solvents. Table 3 shows that for the H1, H1′, H4, H4′, H2, H3, H6, and H7 nuclei the experimental $a^{iso}(^1H)$ values increase when going from methanol to DMSO. Accordingly, the computed values also show the same trend. On the other hand, the H5 and H8 $a^{iso}(^1H)$ values are less in DMSO compared to methanol. This trend is also true for the calculated values. Therefore, from all the above results one may conclude that the addition of NaOH to DHAQ in methanol produces the corresponding DHASQ radical anion.

When DHASQ is subjected to trace amounts of O_2, the solution turns red, and a new species is formed. The EPR spectrum of this solution reveals that, in conjunction with the DHASQ radical, the ASQ radical is also present in significant amounts. Consequently, O_2 has oxidized the DHASQ to the ASQ radical whereby the H1′ and H4′ have been eliminated.

Further increase in the O_2 concentration converts the ASQ radical anion to the neutral AQ molecule. Upon evaporation of the solvent the product quinone is precipitated. Its mass spectrum shows that the most intense peak occurs at 207.4 amu/*z*, and its fragmentation pattern was found to be identical to that of 1,9-anthraquinone. Thus, it is safe to conclude that the final product is the 9,10-anthraquinone.

Finally, the use of NMR, EPR, X-ray diffraction, and mass spectroscopy suggests that the THAQK to AQ reaction follows the set of reactions given in Scheme 4.

4. Summary and Conclusions

The structures of *cis*THAQK obtained by X-ray crystallography and geometry optimization show that their bond lengths and angles are very close. Consequently, the UB1LYP/6-31G-(d) method predicts the experimental solid state geometry quite well.

An important aspect of the THAQK structure, whether determined by calculations or X-ray crystallography, is that both the H11 and H12 protons are on the same side of the molecule.

To determine the THAQK molecular structure in various solvents, one has to resort to 2-D NMR experiments such as $^1H-^{13}C$ HMQC and $^1H-^{13}C$ HMBC. At ambient temperatures, the THAQK is found to fluctuate between two extreme bent configurations resulting in the average structure illustrated in Scheme 1.

When a very small amount of NaOH is added to THAQK in methanol-d_4, it is gradually converted into the corresponding enol form, THAQE. Monitoring this process, by ^1H NMR spectroscopy, reveals that after 72 h the conversion of THAQK to THAQE is complete.

If more NaOH is added such that the NaOH/THAQK ratio is 1:4, a paramagnetic free radical species in solution is formed which is characterized by EPR spectroscopy as the DHASQ radical anion. Therefore, THAQK is first converted to THAQE, and in the presence of more OH^-, it is then further converted into the DHASQ radical anion.

The DHASQ anion may be formed from THAQE via two possible routes shown in Scheme 3. In one, THAQE is converted to give DHAQ which, in turn, is reduced to yield the DHASQ radical anion. In the other, the THAQE is reduced to the DHAQ dianion and is then oxidized back to the DHASQ radical anion. The first mechanism was shown to occur by isolating the DHAQ intermediate, under carefully controlled conditions, and characterizing it by X-ray diffraction. Its solution was then reduced by NaOH to DHASQ and detected by EPR spectroscopy.

The DHASQ radical anion EPR spectra have different splittings patterns and intensities in different solvents such as methanol and DMSO. Consequently, the proper way to compare this radical in various solvents is to simulate its experimental EPR spectra and compare their hyperfine coupling constants obtained from the simulations.

The $a^{iso}(^1H)$ hyperfine coupling constants of DHASQ were computed using the UB1LYP hybrid density functional method. As the effects of the methanol and DMSO solvents are included, the already good agreement between the computed and experimental values in the gas phase gets even better. In addition, the change in the magnitude of the experimental and calculated $a^{iso}(^1H)$ in different solvents follows the same trends.

When the DHASQ radical anion comes in contact with trace amounts of O_2, it is converted into the ASQ radical by elimination of its H1′ and H4′ atoms. Further increase in O_2 concentration totally converts the ASQ radical anion to the neutral AQ molecule.

Having determined the mechanism of the conversion of THAQ into AQ, one is now in a position to understand why the addition of THAQ to alkaline soda-pulping solutions has similar effects to the AQ catalyst in the AQ−soda process. From the present study, it is clear that the alkaline conditions of soda-pulping and the presence of dissolved O_2 in the pulping solutions will convert the THAQ catalyst into AQ as shown in Scheme 4. Thus, THAQ−soda pulping in the presence of atmospheric O_2 is, for all practical purposes, AQ−soda pulping.

Acknowledgment. S.M.M. acknowledges the Natural Sciences and Engineering Research Council of Canada for an operating (Discovery) grant. A.H.E. is grateful to the University of New Brunswick for graduate teaching and research assistantships. The authors would also like to thank Dr. Andreas Decken and Professor T. Stanley Cameron for acquiring the X-ray diffraction data and Mr. Gilles Vautour for the recording of the AQ mass spectra.

Supporting Information Available: Table listing the X-ray and geometry optimized bond lengths [Å] and angles [deg] of *cis*THAQK. This material is available free of charge via the Internet at http://pubs.acs.org.

References and Notes

(1) Mattar, S. M. Ph.D. Thesis, McGill University, 1982.
(2) Mattar, S. M.; Sutherland, D. *J. Phys. Chem.* **1991**, *95*, 5129.
(3) Mattar, S. M.; Sammynaiken, R.; Stephens, A. D. *J. Phys. Chem.* **1997**, *101*, 8227.
(4) Mattar, S. M.; Stephens, A. D. *Chem. Phys. Lett.* **1999**, *306*, 249.
(5) Holton, H. H. (Canadian Industries Limited) U.S. Patent 4,012,-280, March 15, 1977.
(6) Samuelson, O.; Sjoberg, L. A. *Cellul. Chem. Technol*. **1978**, *12*, 463.
(7) Fullerton, T. J.; Ahern, S. P. *J. Chem. Soc., Chem. Commun*. **1979**, 457.
(8) Landucci, L.; Ralph, J. *J. Org. Chem.* **1982**, *47*, 3486.
(9) Hocking, M. B.; Mattar, S. M. *J. Magn. Reson.* **1982**, *47*, 187.
(10) Mattar, S. M.; Fleming B. I. *Tappi* **1981**, *64*, 136.
(11) Doyle, J. E.; Looney, F. D. *Appita* **1982**, *36*, 219.
(12) Ohtani, Y.; Takuro, N.; Kazuhiko, S. *Sen'i Gakkaishi* **1996**, *52*, 175. Ljungquist, P.; Sjoholm, E. *STFI-KONTAKT* **2003**, December Issue, 9.
(13) Tatsuyoshi, K.; Yukio, N.; Hiroaki, T. *Jpn. Kokai* **1976**, *54*, 540.
(14) Al, van T. *Appita* **2000**, *53*, 300.
(15) Jahan, S. M.; Farouqui, F. I. *IPPTA* **2000**, *12*, 15.
(16) Shaka, A. J.; Keeler, J.; Frenkiel T.; Freeman, R. *J. Magn. Reson*. **1983**, *52*, 335.
(17) Mattar, S. M.; Stephens, A. D. *Chem. Phys. Lett.* **2001**, *347*, 189.
(18) Mattar, S. M.; Stephens, A. D.; Emwas, A. H. *Chem. Phys. Lett.* **2002**, *352*, 39.
(19) Mattar, S. M.; Sammynaiken, R. *J. Chem. Phys.* **1997**, *106*, 1080.
(20) Mattar, S. M.; Sammynaiken, R. *J. Chem. Phys.* **1997**, *106*, 1094.
(21) Mattar, S. M.; Stephens, A. D. *Chem. Phys. Lett*. **2001**, *347*, 189.
(22) Frisch, M. J.; Trucks, G. W.; Schlegel, H. B.; Scuseria, G. E.; Robb, M. A.; Cheeseman, J. R.; Zakrzewski, V. G.; Montgomery, J. A., Jr.; Stratmann, R. E.; Burant, J. C.; Dapprich, S.; Millam, J. M.; Daniels, A. D.; Kudin, K. N.; Strain, M. C.; Farkas, O.; Tomasi, J.; Barone, V.; Cossi, M.; Cammi, R.; Mennucci, B.; Pomelli, C.; Adamo, C.; Clifford, S.; Ochterski, J.; Petersson, G. A.; Ayala, P. Y.; Cui, Q.; Morokuma, K.; Malick, D. K.; Rabuck, A. D.; Raghavachari, K.; Foresman, J. B.; Cioslowski, J.; Ortiz, J. V.; Stefanov, B. B.; Liu, G.; Liashenko, A.; Piskorz, P.; Komaromi, I.; Gomperts, R.; Martin, R. L.; Fox, D. J.; Keith, T.; Al-Laham, M. A.; Peng, C. Y.; Nanayakkara, A.; Gonzalez, C.; Challacombe, M.; Gill, P. M. W.; Johnson, B. G.; Chen, W.; Wong, M. W.; Andres, J. L.; Head-Gordon, M.; Replogle, E. S.; Pople, J. A. *Gaussian 98*, revision A.3; Gaussian, Inc.: Pittsburgh, PA, 2003.
(23) Adamo, C.; Barone, V.; Fortunelli, V. *J. Chem. Phys.* **1995**, *102*, 1689.
(24) Adamo, C.; Barone, V. *Chem. Phys. Lett*. **1997**, *274*, 214.
(25) Barone, V. In *Advances in Density Functional Methods*; Chong, D. P., Ed.; World Scientific Publishing: Singapore, 1995.
(26) O'Malley, P. J. *Chem. Phys. Lett.* **1998**, *285*, 99.
(27) di Matteo, A.; Adamo, C.; Cossi, M.; Barone, V.; Rey, P. *Chem. Phys. Lett*. **1999**, *310*, 159.
(28) Barone, V.; Cossi, M.; Tomasi, J. *J. Chem. Phys.* **1997**, *107*, 3210.
(29) Adamo, C.; di Matteo, A.; Rey, P.; Barone, V. *J. Phys. Chem. A* **1999**, *103*, 3481.
(30) Mattar, S. M.; Emwas, A. H.; Decken, A.; Cameron, T. S. *Acta Crystallogr., Sect. E*, submitted.
(31) Phillips, S. E.; Trotter, J. *Acta Crystallogr*. **1977**, *B33*, 1605.
(32) Wu, G.; Zheng, P. *Acta Crystallogr., Sect. C* **1991**, *C47*, 1227.
(33) Chy, S. C. *Acta Crystallogr., Sect. B* **1976**, *B32*, 1583.